

Recovering vertical and time-dependent deformation near Coachella Valley, California with InSAR

Report for SCEC Award #15108

Submitted on March 14, 2016

Investigators: David Schmidt (University of Washington), Xiaopeng Tong (University of Washington),
Andrew Barbour (USGS Menlo Park), David Sandwell (UCSD)

| | |
|--|----|
| I. Project Overview..... | i |
| A. Abstract..... | i |
| B. SCEC Annual Science Highlights..... | i |
| C. Exemplary Figure..... | ii |
| D. SCEC Science Priorities..... | ii |
| E. Intellectual Merit..... | ii |
| F. Broader Impacts..... | ii |
| G. Project Publications..... | ii |
| II. Technical Report..... | 1 |
| A. Technical Report | |
| 1. Objectives | |
| 2. Methods | |
| 3. Results | |
| 4. Discussion and Conclusions | |
| B. References | |

I. Project Overview

A. Abstract

In the box below, describe the project objectives, methodology, and results obtained and their significance. If this work is a continuation of a multi-year SCEC-funded project, please include major research findings for all previous years in the abstract. (Maximum 250 words.)

This study focuses on analyzing the SAR data in Southern California with the goal of resolving the surface deformation found along the Southern San Andreas fault. We present a refined methodology for recovering the time-dependent deformation that enhances the signal in regions of low coherence. Our InSAR time-series method incorporates pixel coherence into the covariance matrix, which performs better than the traditional Small Baseline Subset (SBAS) method. We analyzed ERS, ENVISAT and ALOS-1 data over the Coachella Valley region with this coherence-based SBAS method. The InSAR maps show many interesting deformation signals including (1) post-seismic transient from 1992 Landers and 1999 Hector Mine earthquakes, (2) aquifer deformation near the San Andreas Fault and the San Jacinto Fault, (3) the compliant fault zone of the Pinto Mountain fault. These results provide higher resolution images of these geodetic signals. Anomalies in the vertical deformation field, at the southwestern edge of the Coachella Valley, can be explained by fluid extraction from a

poroelastic half-space model. To reduce the atmospheric noise in the InSAR measurements, we propose a new way to determine an optimal temporal smoothing factor. The choice of the smoothing can be determined by investigating the empirical trade-off between the RMS reduction of the phase of the interferograms and the smoothing weight. The results are in good agreement with vertical GPS time-series.

B. SCEC Annual Science Highlights

Each year, the Science Planning Committee reviews and summarizes SCEC research accomplishments, and presents the results to the SCEC community and funding agencies. Rank (in order of preference) the sections in which you would like your project results to appear. Choose up to 3 working groups from below and re-order them according to your preference ranking.

Tectonic Geodesy

Stress and Deformation Through Time (SDOT)

Aseismic Transient Detection

C. Exemplary Figure

Select one figure from your project report that best exemplifies the significance of the results. The figure may be used in the SCEC Annual Science Highlights and chosen for the cover of the Annual Meeting Proceedings Volume. In the box below, enter the figure number from the project report, figure caption and figure credits.

Figure 3. a) InSAR mean velocity from ENVISAT (2003-2011) over the Coachella Valley in Southern California. b) Comparison between the relative displacement time-series of GPS and InSAR at sites COTD and sites PSAP. c) Similar comparison as b) at sites CACT and sites TMAP. d) The subsidence observed by InSAR near COTD (left), a model of fluid extraction from a poroelastic half-space (middle), and residual displacements (right). The best-fitting extraction rates and depths for the five sources along the profile (at the dashed lines) are found by Simulated Annealing. (Figure credits: X. Tong, A. Barbour, D. Schmidt, D. Sandwell).

D. SCEC Science Priorities

In the box below, please list (in rank order) the SCEC priorities this project has achieved. See <https://www.scec.org/research/priorities> for list of SCEC research priorities. *For example: 6a, 6b, 6c*

1d, 4a, 5b

E. Intellectual Merit

How does the project contribute to the overall intellectual merit of SCEC? *For example: How does the research contribute to advancing knowledge and understanding in the field and, more specifically, SCEC research objectives? To what extent has the activity developed creative and original concepts?*

This research helps to resolve the interseismic deformation across the plate boundary, which is directly related to the strain accumulation on regional faults. We further developed an important geodetic method for producing InSAR time-series. Tests on multiple InSAR dataset have shown the capability of this approach to retrieve surface deformation, especially in the vertical direction. This research advances our understanding of time-varying geodetic signals in Southern California especially in the vertical component. A reliable vertical displacement field can help us to develop both the time-dependent and time-independent component of the CGM.

F. Broader Impacts

How does the project contribute to the broader impacts of SCEC as a whole? *For example: How well has the activity promoted or supported teaching, training, and learning at your institution or across SCEC? If your project included a SCEC intern, what was his/her contribution? How has your project broadened the participation of underrepresented groups? To what extent has the project enhanced the infrastructure for research and education (e.g., facilities, instrumentation, networks, and partnerships)? What are some possible benefits of the activity to society?*

The funding of the project has supported a postdoc at University of Washington and his collaborations with scientists from the University of California San Diego and the USGS. The development of the InSAR time-series method is implemented in an open source InSAR processing system. The results of this research have been presented at the SCEC annual meeting.

G. Project Publications

All publications and presentations of the work funded must be entered in the SCEC Publications database. Log in at <http://www.scec.org/user/login> and select the Publications button to enter the SCEC Publications System. Please either (a) update a publication record you previously submitted or (b) add new publication record(s) as needed. If you have any problems, please email web@scec.org for assistance.

Tong X., D. Schmidt, A. Barbour, D. Sandwell, A coherence-based small-baseline subset method for InSAR with applications to the Coachella Valley, California, *SCEC annual meeting 2015*, Palm Springs, CA.

Tong X., E. Lindsey, D. Sandwell, Y. Fialko, B. Smith-Konter, B. Crowell, S. Baker, A preliminary Community Geodetic Velocity Model of the San Andreas Fault System from GPS and InSAR, *SCEC annual meeting 2015*, Palm Springs, CA.

Tong X., E. Lindsey, D. Sandwell, Y. Fialko, B. Smith-Konter, Merging GPS and InSAR for uniform velocity, *SCEC CGM workshop 2016*, Pomona, CA.

II. Technical Report

A. Project summary

We investigated the time-varying geodetic signals in the vicinity of Coachella Valley using an InSAR time-series method. The completed tasks include:

- Produced a time-averaged line-of-sight velocity map and InSAR time-series by applying the coherence-based SBAS analysis to multiple SAR satellite data sets.
- Determined an optimal temporal filter for retrieving time-dependent deformation signals.
- Compared InSAR-derived time-series with the GPS time-series.
- Developed a poroelastic model that explains the first-order feature of the time-dependent aquifer deformation in the western Coachella Valley as a result of anthropogenic activities (aquifer depletion).

1. Objective

Our goals were to 1) contribute to the development of the Community Geodetic Model (CGM) by analyzing the existing SAR data over Southern California; 2) characterize the time-dependent geodetic signal arising from hydrological anomalies, with a focus on the Coachella Valley; 3) improve upon InSAR data analysis methodologies. Using the archived SAR data from recent satellite missions, we constructed a time-averaged velocity map by analyzing a large volume of SAR data from ERS-1/2, ENVISAT, and ALOS-1 missions. Constructing longer time-series data products allows us to 1) reduce the uncertainty of the long-term velocity measurements from InSAR and 2) better characterize and understand vertical deformation signals. We participated in multiple workshops and telecons with other members of the CGM, including the InSAR time-series comparison exercise.

2. Methods

InSAR observations have been used successfully to resolve details in the interseismic surface velocity field. However, the InSAR coherence is significantly compromised in vegetated and cultivated regions, leaving the active deformation within those areas unmapped. Here we developed a modified method of producing InSAR time series that enhances the recovered signal in decorrelated regions.

We have improved the conventional small-baseline subset (SBAS) method [Bernardino *et al.*, 2002; Schmidt and Burgmann, 2003] by introducing coherence of the interferograms into the inverse problem. Instead of discarding those pixels where one or more of the interferograms are incoherent, we keep all the pixels in the processing chain and design a covariance matrix based on the coherence in each interferogram. This coherence-based SBAS method results in a deformation map that is more spatially continuous than the conventional approach, and helps to better constrain the deformation across the plate boundary (Figure 1). To further refine the SBAS-InSAR products, we also apply an elevation-dependent correction to the derived InSAR velocity map to take into account any remaining atmospheric artifacts, which helps to further enhance any deformation signals. In the time series inversion, a damping term is typically included which acts to smooth the InSAR time series; we find the optimal results by exploring the dependence of the RMS reduction of the phase of the interferograms, DEM error, and mean velocity on the smoothing factor. The weighted least-squares inversion that operates on each phase pixel is:

$$W \begin{bmatrix} 1 & 1 & 0 & \dots & \beta B_1 \\ 0 & 1 & 1 & \dots & \beta B_2 \\ \dots & \dots & \dots & \dots & \dots \\ \lambda & -\lambda & 0 & \dots & 0 \\ 0 & \lambda & -\lambda & \dots & 0 \end{bmatrix} \begin{bmatrix} m_1 \\ m_2 \\ \dots \\ m_i \\ \Delta h \end{bmatrix} = W \begin{bmatrix} d_1 \\ d_2 \\ \dots \\ 0 \\ 0 \end{bmatrix} \quad (1)$$

$$W = \text{diag}\{\gamma_1, \gamma_2, \gamma_3, \dots, \gamma_n\} \quad (2)$$

All variables are defined in Table 1. The data kernel matrix has size of $[n \times s+1]$, where n is the number of interferograms and s is the number of temporal increments. When selecting interferograms in the SBAS analysis, we used liberal criteria: the temporal baseline is smaller than 700 days and the spatial baseline is smaller than 300 m. We solved the inverse problem (Equation 1) on a pixel-by-pixel basis to obtain the final InSAR time-series of the cumulative line-of-sight displacement $M(t)$, such that $M(t)$ is the cumulative sum of m_i . The algorithm is implemented as a C-program called *sbas* inside GMTSAR and is publicly available.

Table 1. Definition for equation (1) and (2).

| Symbol | Meaning |
|------------|---|
| m_i | Incremental displacement for each epoch |
| d_i | LOS phase of the <i>i</i> th inteferogram |
| B_i | Perpendicular baseline of the <i>i</i> th interferogram |
| β | Scale factor determined by radar wavelength, the incidence angle of the radar wave, and the distance from the radar to the ground |
| W | Diagonal matrix containing coherence weights |
| γ_i | Coherence of the <i>i</i> th interferogram |
| Δh | DEM error |
| λ | Smoothing factor |

We have investigated the choice of the optimal temporal smoothing factor (λ) in detail (see Figure 2). Variations in the atmosphere and the ionosphere are the greatest sources of error in the deformation signal from InSAR. Temporal and spatial filtering can be employed to mitigate these errors, and we investigated the optimal temporal filters for the InSAR time-series analysis. The phase measurements from InSAR can be decomposed into three main components: atmospheric delay, deformation, and errors in the Digital Elevation Model (DEM). The deformation and the errors in the DEM can be independently resolved. The amplitude of the atmosphere component can be quantified by the root-mean-square (RMS)

of the phase residuals. The RMS reduction is defined as the ratio of the RMS of the phase residuals and the RMS of the original phase data. We are interested in establishing an empirical relationship between the temporal smoothing and the RMS reduction of the InSAR phase components. This relationship would then guide our choice in determining the optimal temporal smoothing for estimating the time-varying signals.

We process raw SAR data to form individual interferograms using a batch processing method [Tong *et al.*, 2013]. From the interferograms, we used the new coherence-based Small-Baseline Subset method to compute InSAR time-series on a pixel-by-pixel basis. The mean velocity represents a linear fit through each time-series. We then corrected the phase ramps with the remove/restore method with constraints from GPS [Smith-Konter *et al.*, 2011].

GPS sites are usually located in regions with less vegetation in order to avoid multi-paths effects. There are 4 continuous GPS sites near the Coachella Valley (COTD, PSAP, TMAP, CACT) that have long time-series. Three GPS sites in the sedimentary basin are susceptible to groundwater disturbance. The correlation of coherent phase pixels and the GPS sites is investigated by comparing the InSAR results to the GPS data.

3. Results

We applied this improved InSAR time-series method to ERS-1/2 and ENVISAT and ALOS-1 data near the Coachella Valley, California, where agricultural parcels and golf courses are prevalent. The mean velocity from ERS-1/2 (Track 127) with and without the coherence-weighting is demonstrated in Figure 1. A clear improvement in the mean Line-Of-Sight (LOS) velocity estimation can be seen. The standard deviation of the velocity map reduces from 2.9 mm/yr to 2.6 mm/yr. The patchiness in the right-panel of Figure 1 is caused by the decorrelation in a fraction of the interferograms. These outliers bias the linear regression analysis of the time-series data. With the new method, we derived a clearer image of the mean velocity field. We did a similar test on the ENVISAT data (Track 77). However, the improvements to the ENVISAT data is less significant than that found for the ERS data. We suspect that this is because the ERS data contain much more decorrelation than the ENVISAT data.

There are several interesting deformation signals resolved in the InSAR data (Figure 1a). While many of these signals have been identified in previous studies, our InSAR products show an improved signal-to-noise ratio. Discontinuities in the high-resolution velocity map reveal the surface trace of the Coachella section and the San Bernardino section of the San Andreas fault, the Garnet Hill fault, and the San Jacinto fault zone [Wisely and Schmidt, 2010]. In the Coachella Valley, the InSAR velocity map captures deformation that can be attributed to the aquifer's response to the withdrawal of fluid. The northern part of the Coachella Valley region is subsiding at average rates of 5-10 mm/yr from 1992-2000, with the subsidence diminishing along the western edge of the Coachella Valley from 2003-2010 (Figure 3a). The subsidence near Palm Desert is bounded by a lineament lying parallel to the San Andreas fault, which could indicate that a buried fault in the Coachella Valley is acting as an impermeable boundary to fluid flow. Near the Palm Desert region the mean velocity from InSAR reveals four pockets of localized subsidence areas. The maximum subsidence rate reaches about 4 cm/yr.

There is a clear subsidence region distributed along the Pinto Mountain fault. Fialko *et al.* [2002] identified the Pinto Mountain fault to be a compliant fault zone that responded to the stress changes from nearby earthquakes. There is a prominent uplift area near the Johnson Valley fault as well as the northern terminus of the Burnt Mountain fault. Peltzer *et al.* [1998] explained this uplift pattern as caused by the

poroelastic response of the fluid-filled crust after the 1992 Landers earthquake. The InSAR data has revealed an area of subsidence within the San Jacinto fault zone near the city of San Jacinto, bounded by the Casa Loma fault and the Claremont fault..

To choose an optimal temporal filter in the InSAR time-series analysis we investigated the dependence of the mean velocity, DEM error, and the RMS reduction on the smoothing factor (Figure 2). We have experimented with five different smoothing weights, from no smoothing ($\lambda=0$) to strong smoothing ($\lambda=500$). The estimation of the mean velocity did not change significantly for $\lambda>0.5$. The estimation of the DEM error is also quite robust for $\lambda>0.5$. The range of the DEM error is generally less than 10 m. The RMS reduction provides us with diagnostics of the optimal smoothing factor. Using too little or too much smoothing results in a small reduction in RMS. To fully account for the phase information from interferograms, we find acceptable smoothing weights from 0.5-10. A typical value of the RMS reduction can reach above 40% for most of the pixels. The rest of the phase is noise, which comes mainly from temporal variations of the atmosphere. In the final analysis of the ERS and ENVISAT data, we chose a smoothing weight of 5.

We compared the InSAR-derived time series with GPS daily position (unfiltered) solution at sites PSAP and COTD, CATC and TMAP (Figure 3b and 3c). The GPS data is from UNAVCO (PBO solution) and it is projected into the radar line-of-sight direction to compare with InSAR (ENVISAT) data. The horizontal and the vertical component of the GPS displacement are projected separately, to better visualize how they independently contribute to the line-of-sight signal in the InSAR. It is evident that the variability we see from both GPS and InSAR time-series data are primarily from the vertical displacement. Horizontal displacement of the GPS sites are negligible when projected into the line-of-sight given that we are trying to resolve the variation in deformation at a spatial scale of less than ~ 10 km. A good agreement is found between GPS and InSAR. The misfit is at the mm-level in the trend of the time-series. This misfit could reflect the spatial smoothing in the InSAR data. When extracting the time-series data at a specific GPS location, we have applied a spatial Gaussian filter with a 2 km window size on the InSAR data.

Our goal is to image a complete inter-seismic velocity and strain field along the plate boundary. To better model and remove the subsidence signal from the tectonic deformation in the western Coachella Valley, we developed a poroelastic model based on effective mass loss from a horizontally extensive permeable layer [i.e., *Segall*, 1985]. We use the “best-fitting” fluid-extraction rates, obtained using a Simulated Annealing non-linear inversion technique, in a numerical simulation of fluid extraction from a layered half-space [e.g., *Barbour and Wyatt*, 2014]. The results from a layered solution are not that different from a homogeneous half-space solution, and in both cases, we find that subsidence observed by InSAR (near COTD) is well explained by this modeled fluid-extraction within the localized subsidence basin. The location of the data profile is marked in Figure 3a, and the best-fitting model is demonstrated in Figure 3d; it consists of 5 sources with different locations and various fluid extraction rates.

4. Discussions and conclusions

The InSAR time-series method we developed helps to recover deformation in the decorrelated regions in Southern California. This coherence-based SBAS method has proven to be effective on both the L-band ALOS-1 and C-band ERS and ENVISAT data. The geodetic results from ERS and ENVISAT span the 1992 Landers and 1999 Hector Mine earthquake, and we observed clear postseismic transient signals, both along Landers rupture and on nearby compliant fault zones.

The widespread hydrological signals imaged by InSAR appear to match the geometry of sub-surface fault branches. This implies that changes in the hydrologic system from anthropogenic fluid extraction may have a direct influence on shallow fault processes, including changes in effective normal stress by variations in pore pressure. In this case, an accurate poroelastic model for aquifer depletion can help place bounds on the hydraulic diffusivity and elastic shear modulus of rock near the fault zone [e.g., *Barbour and Wyatt, 2014*], and help remove the effects of non-tectonic sources from the deformation time series.

This study has demonstrated a good agreement between the GPS and InSAR observations. The discrepancies are likely to be caused by vertical displacements. A reliable vertical displacement field can help us to develop the time-dependent CGM, which will provide a steady-state interseismic reference velocity model for the search of aseismic transient signals over Southern California.

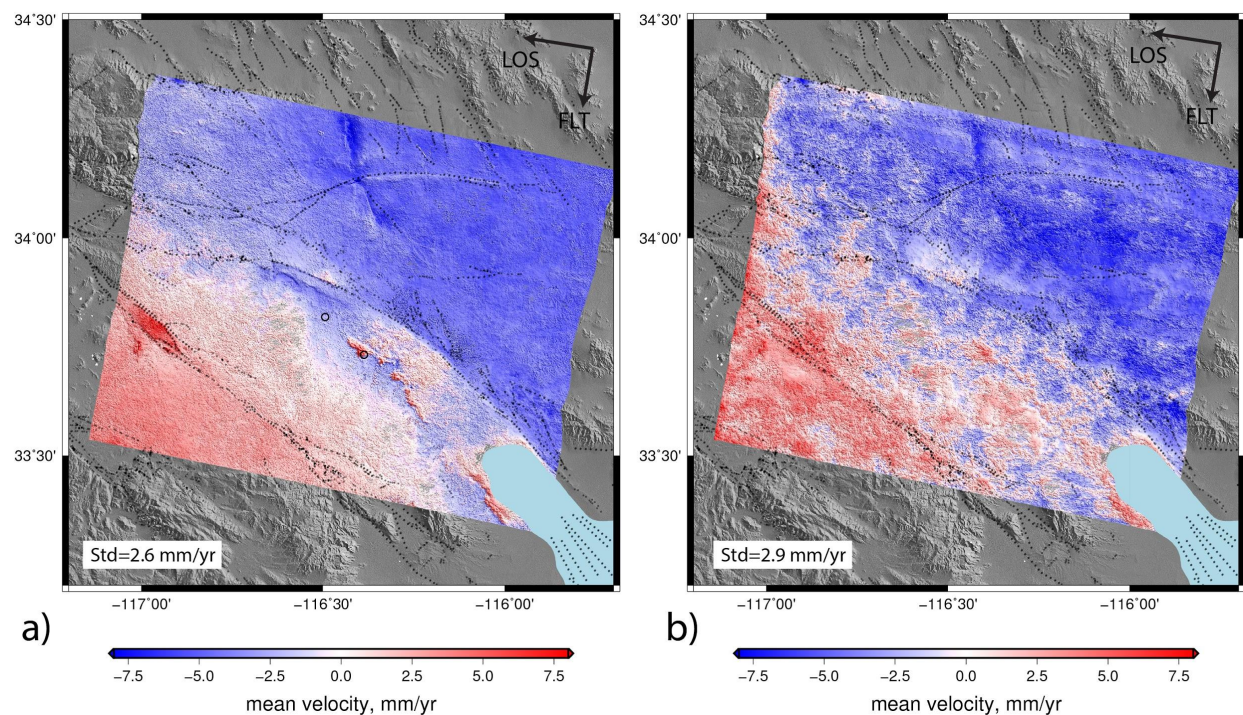


Figure 1. Mean LOS velocity constructed by two different methods. A) Coherence-based SBAS; B) SBAS with uniform weights. The data set is from ERS-1 and ERS-2 (1992-2001). Red means ground moving away from satellite and blue means ground moving toward satellite. Major fault segments are marked by black dots. The standard deviation of the mean velocity is denoted in the bottom of the figure.

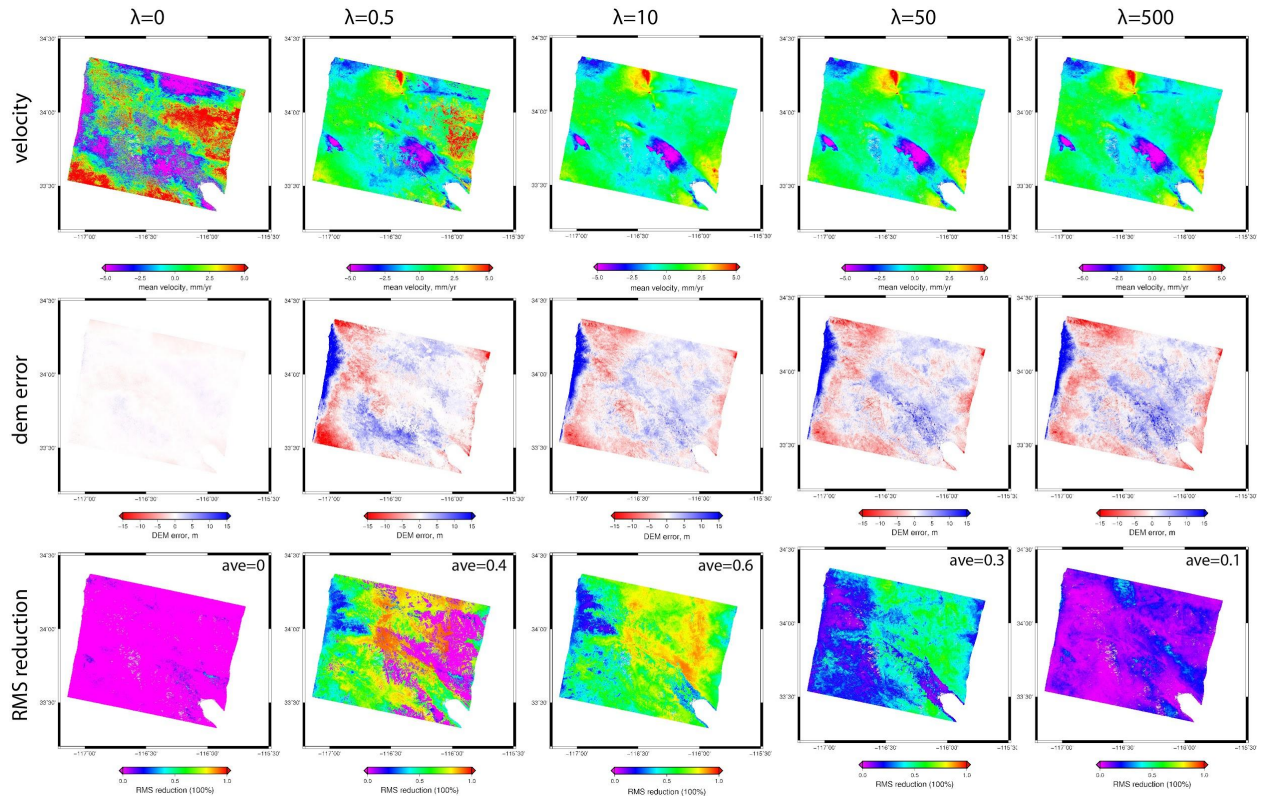


Figure 2. Effects of smoothing factor (λ) on mean velocity, DEM error and RMS reduction. The data set is from ERS-1 and ERS-2 (1992-2001). Smoothing factor of 0, 0.5, 10, 50, 500 are considered in this test. To demonstrate the effect of the smoothing on the mean velocity we didn't include the remove/restore correction with the GPS data. Red corresponds to uplift and blue corresponds to subsidence. In the RMS reduction row, the average RMS reduction (in percentage) is denoted in the upper-right corner.

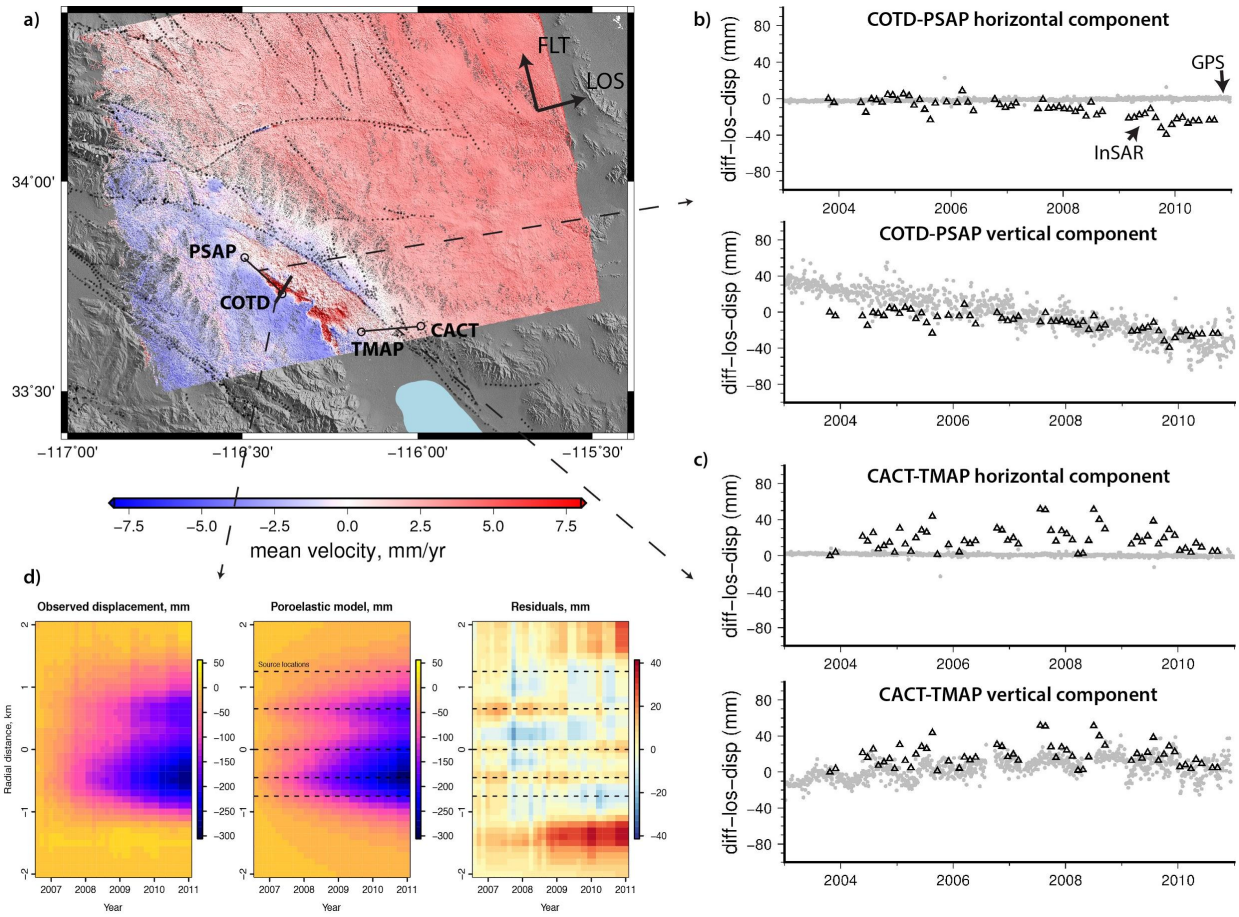


Figure 3. a) InSAR mean velocity from ENVISAT (2003-2011) over the Coachella Valley in Southern California. b) Comparison between the relative displacement time-series of GPS and InSAR at sites COTD and sites PSAP, emphasizing the independent contribution for vertical and horizontal GPS deformation projected onto the InSAR line-of-sight. c) Similar comparison as b) at sites CACT and sites TMAP. d) The subsidence observed by InSAR near COTD (left), a model of fluid extraction from a poroelastic halfspace (middle), and residual displacements (right). The best-fitting extraction rates and depths for the five sources along the profile (at the dashed lines) are found by Simulated Annealing.

B. References

- Barbour, A. J., & Wyatt, F. K. (2014). Modeling strain and pore pressure associated with fluid extraction: The Pathfinder Ranch experiment. *Journal of Geophysical Research: Solid Earth*, 119(6), 5254-5273, doi: 10.1002/2014JB011169.
- Berardino, F., Fornaro, G., Lanari, R., & Sansosti, E. (2002). A new algorithm for surface deformation monitoring based on small baseline differential SAR interferometry. *IEEE Transactions on Geoscience and Remote Sensing*, 40, 2375–2383.
- Fialko, Y. (2004), Evidence of fluid-filled upper crust from observations of postseismic deformation due to the 1992 Mw7.3 Landers earthquake, *J. Geophys. Res.*, 109, B08401, doi:10.1029/2004JB002985.
- Peltzer, G., P. Rosen, F. Rogez, and K. Hudnut (1998), Poroelastic rebound along the Landers 1992 earthquake surface rupture, *J. Geophys. Res.*, 103(B12), 30131–30145, doi:10.1029/98JB02302.
- Tong, X., D. T. Sandwell and B. Smith-Konter (2013), High resolution interseismic velocity data along the San Andreas fault from GPS and InSAR, *J. Geophys. Res.*, 118, doi:10.1029/2012JB009442.
- Segall, P. (1985), Stress and subsidence resulting from subsurface fluid withdrawal in the epicentral region of the 1983 Coalinga earthquake, *Journal of Geophysical Research: Solid Earth*, 90(B8), 6801-6816.
- Schmidt, D. A., and R. Bürgmann (2003), Time-dependent land uplift and subsidence in the Santa Clara valley, California, from a large interferometric synthetic aperture radar data set, *J. Geophys. Res.*, 108 (B9), 2416, doi: 10.1029/2002JB002267.
- Smith-Konter, B., D. T. Sandwell, and P. Shearer (2011), Locking depths estimated from geodesy and seismology along the San Andreas Fault System: Implications for seismic moment release, *J. Geophys. Res.*, 116, B06401, doi:10.1029/2010JB008117.
- Wisely, B. A., and D. Schmidt (2010), Deciphering vertical deformation and poroelastic parameters in a tectonically active fault-bound aquifer using insar and well level data, san bernardino basin, california, *Geophys. J. Int.*, 181(3), 1185–1200, doi:10.1111/j.1365-246X.2010.04568.x.